Supplementary Information

Reactive Metal Boride Nanoparticles Trap Lipopolysaccharide and Peptidoglycan for Bacteria-Infected Wound Healing

Yun Meng[1,2#], Lijie Chen [2#], Yang Chen[1,3#], Jieyun Shi[1], Zheng Zhang[4], Yiwen Wang[4], Fan Wu[2], Xingwu Jiang[2], Wei Yang[1], Li Zhang [1], Chaochao Wang[1], Xianfu Meng[1], Yelin Wu[1*], Wenbo Bu[1,2*]

[1]Tongji University Cancer Center, Shanghai Tenth Peoples Hospital, Tongji University School of Medicine, Shanghai 200072, P. R. China

[2]Department of Materials Science and State Key Laboratory of Molecular Engineering of Polymers, Fudan University, Shanghai 200433, P. R. China

[3] School of Life Sciences and Technology, Tongji University, Shanghai 200092, P. R. China

[4]School of life Science, East China Normal University, Shanghai 200241, P. R. China

[#]These authors contributed equally to this work.

Email: sk_wuyelin@tongji.edu.cn; wbbu@fudan.edu.cn;

Supplementary Information:

Supplementary Figures 1-23

Supplementary Tables 1, 2, 3

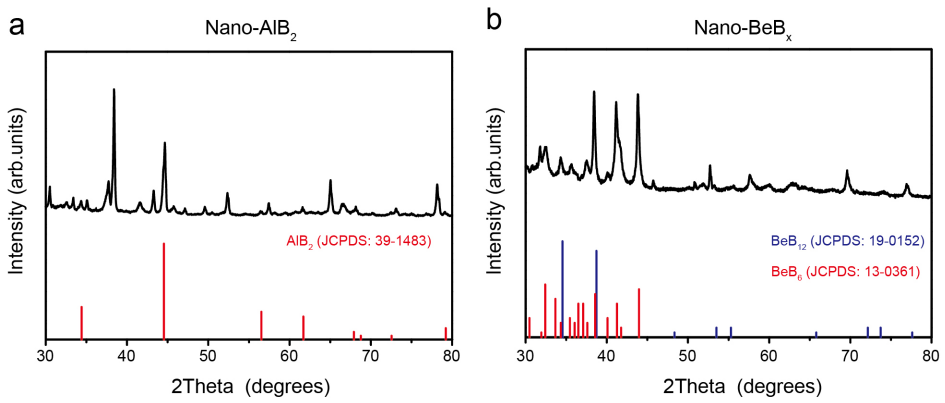

Supplementary Fig. 1 XRD patterns of **a**, Nano-AlB_2 and **b**, Nano-BeB_x. Source data are provided as a Source Data file.

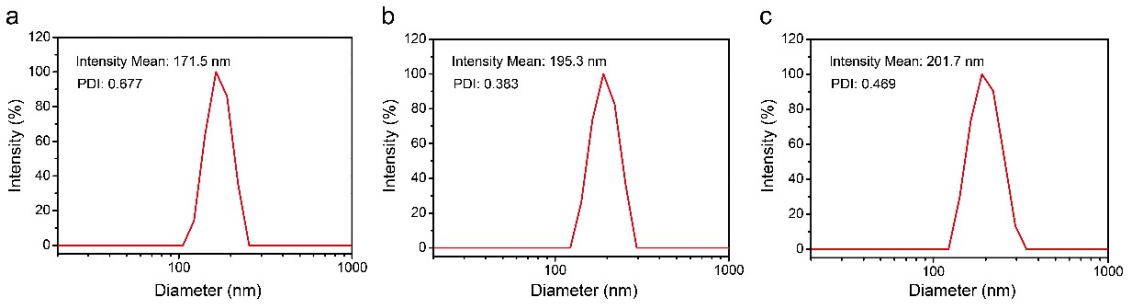

Supplementary Fig. 2 Particle size analysis of **a**, Nano-MgB_2, **b**, Nano-AlB_2 and **c**, Nano-BeB_x. Source data are provided as a Source Data file.

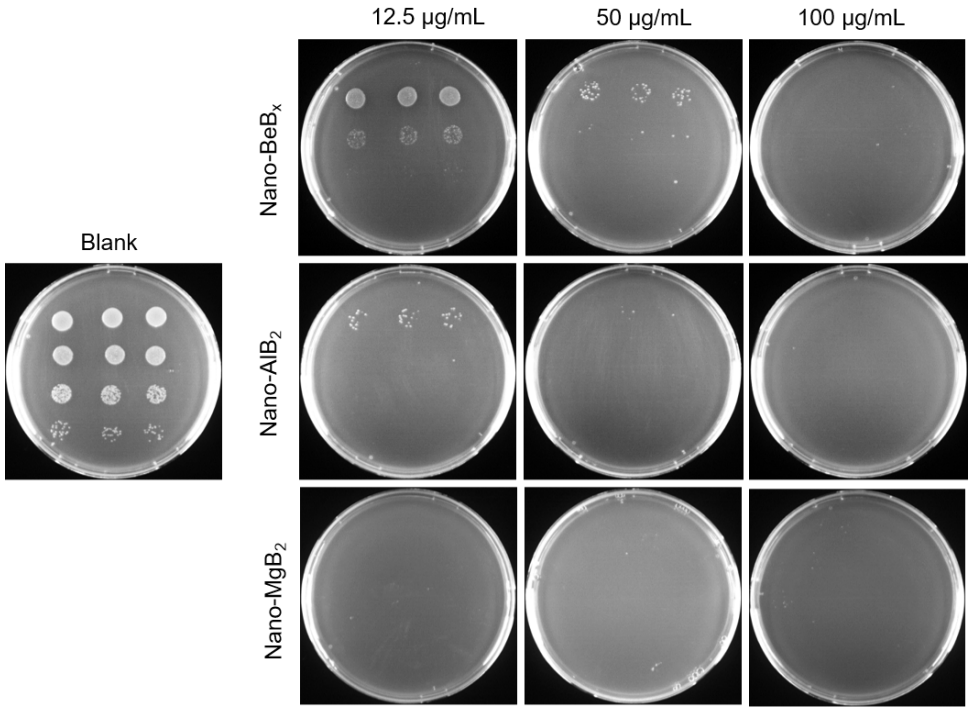

Supplementary Fig. 3 Antibacterial activity of Nano-MgB_2, Nano-AlB_2 and Nano-BeB_x. *P. aeruginosa* treated with different concentrations of Nano-MgB_2, Nano-AlB_2 and Nano-BeB_x (n=3 biological independent cells).

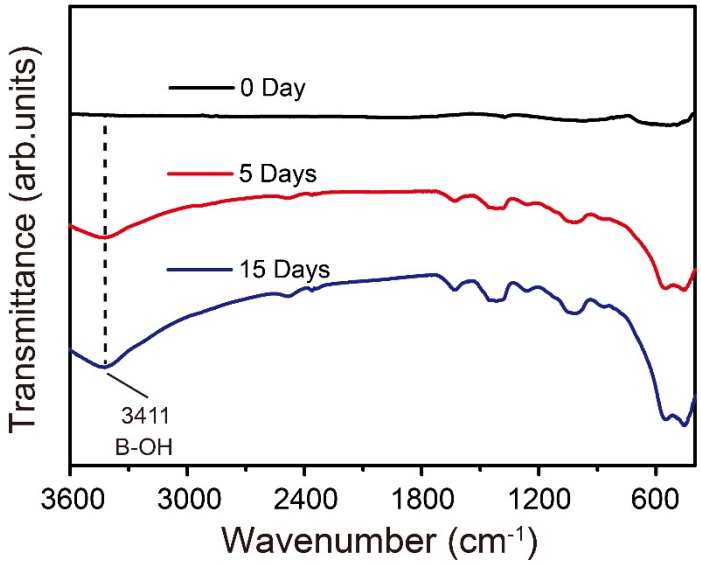

Supplementary Fig. 4 FTIR spectrum analysis of the hydrolysis process of Nano-MgB_2 in 15 days. Source data are provided as a Source Data file.

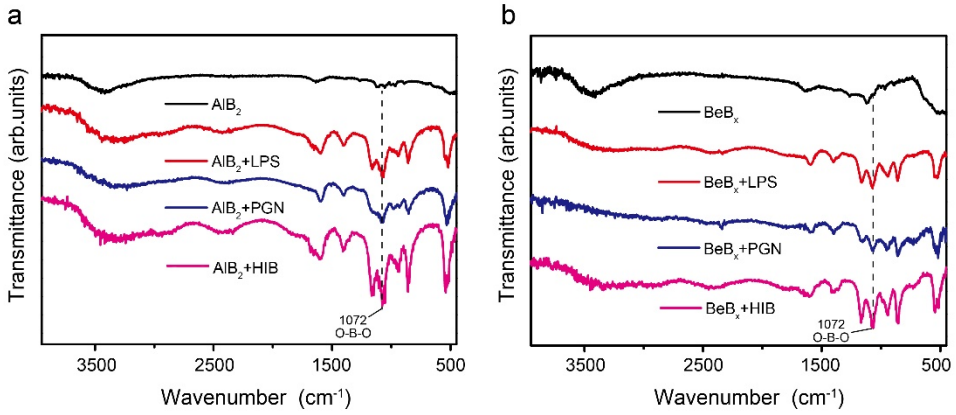

Supplementary Fig. 5 FTIR spectra of O-B-O of **a**, Nano-AlB_2 and **b**, Nano-BeB_x incubated with LPS, PGN, and HIB, respectively. Source data are provided as a Source Data file.

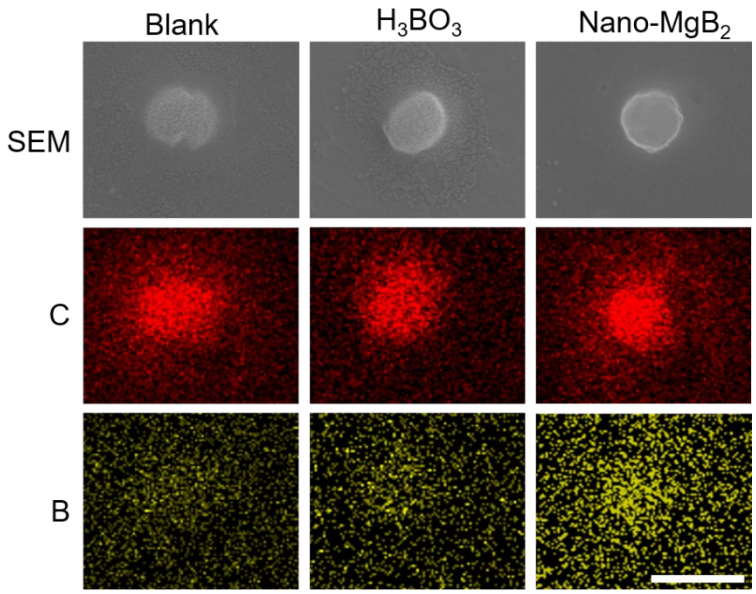

Supplementary Fig. 6 Elemental mapping of *S. aureus* incubated with H_3BO_3 and Nano-MgB_2 for 3 h (scale bar=500 nm). Data are representative of at least three independent experiments with similar results.

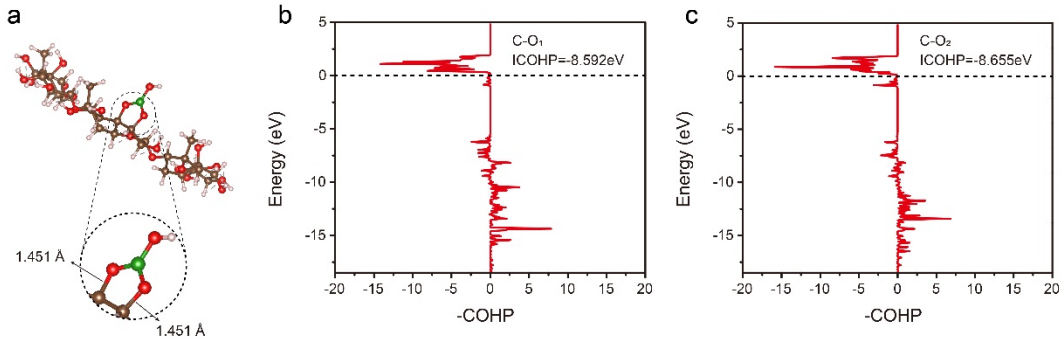

Supplementary Fig. 7 Theoretical simulation for the H_3BO_3-saccharide complexation. **a**, DFT calculations and **b-c**, COHP analysis of C-O_1, C-O_2 bond interactions corresponding to the complexation of H_3BO_3 with the 3, 4-o-hydroxyl groups of bicyclic monosaccharide structure. Source data are provided as a Source Data file.

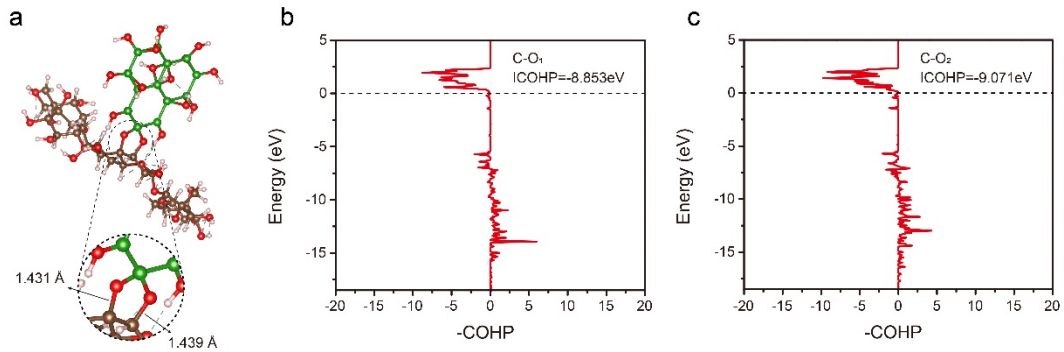

Supplementary Fig. 8 Theoretical simulation for the Nano-MgB_2-saccharide complexation. **a**, DFT calculations and **b-c**, COHP analysis of C-O_1, C-O_2 bond interactions corresponding to the complexation of hydrolysate of Nano-MgB_2 with the 3, 4-o-hydroxyl groups of bicyclic monosaccharide structure. Source data are provided as a Source Data file.

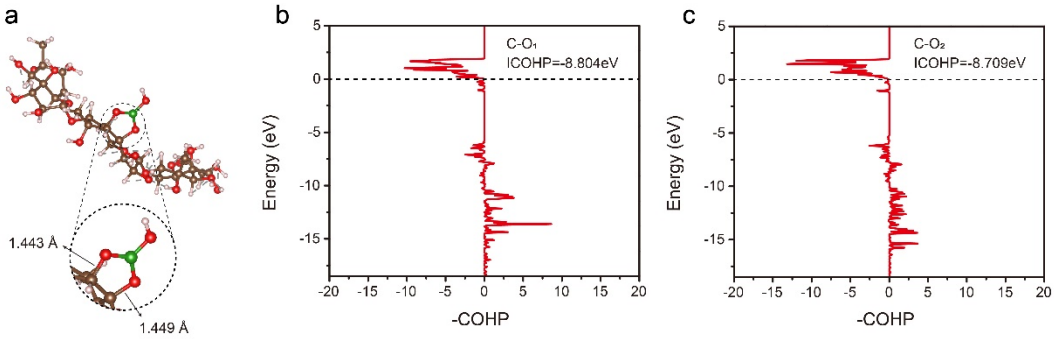

Supplementary Fig. 9 Theoretical simulation for the H_3BO_3-saccharide complexation. **a**, DFT calculations and **b-c**, COHP analysis of C-O_1, C-O_2 bond interactions corresponding to the complexation of H_3BO_3 with the 4, 5-o-hydroxyl groups of bicyclic monosaccharide structure. Source data are provided as a Source Data file.

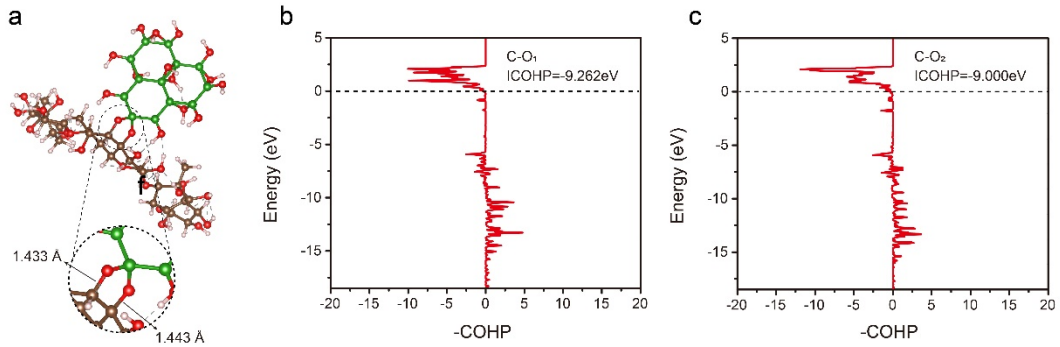

Supplementary Fig. 10 Theoretical simulation for the Nano-MgB_2-saccharide complexation. **a**, DFT calculations and **b-c**, COHP analysis of C-O_1, C-O_2 bond interactions corresponding to the complexation of hydrolysate of Nano-MgB_2 with the 3, 4-o-hydroxyl groups of bicyclic monosaccharide structure. Source data are provided as a Source Data file.

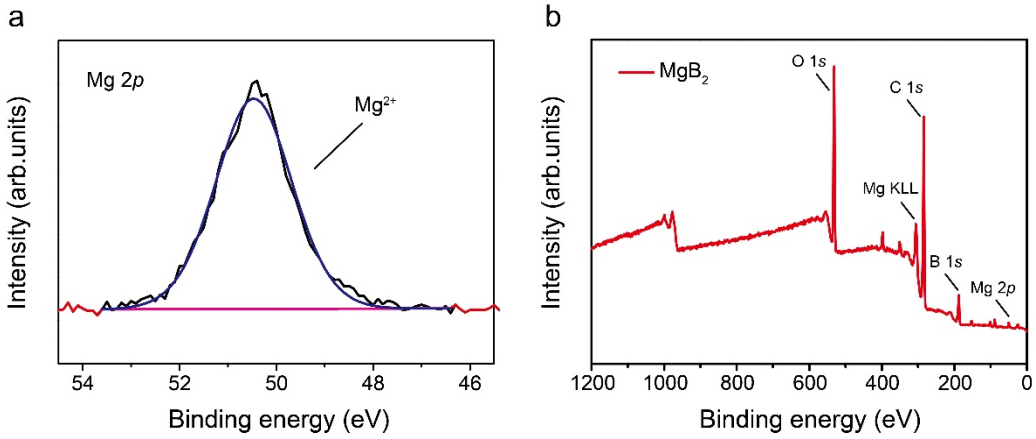

Supplementary Fig. 11 XPS characterization of Nano-MgB_2. **a**, XPS fine spectra of Mg 2*p* signal and **b**, XPS survey spectra of Nano-MgB_2 deconvoluted by the multi-Gaussian function.

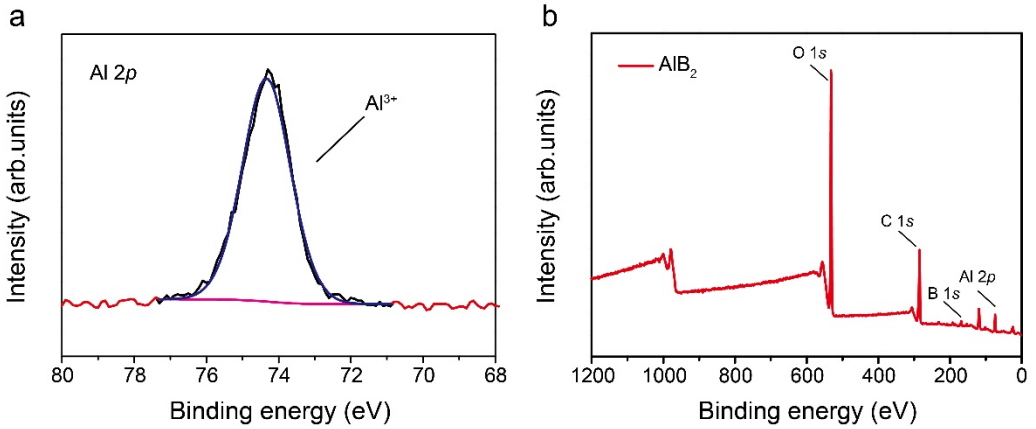

Supplementary Fig. 12 XPS characterization of Nano-AlB_2. **a**, XPS fine spectra of Al 2*p* signal and **b**, XPS survey spectra of Nano-AlB_2 deconvoluted by the multi-Gaussian function.

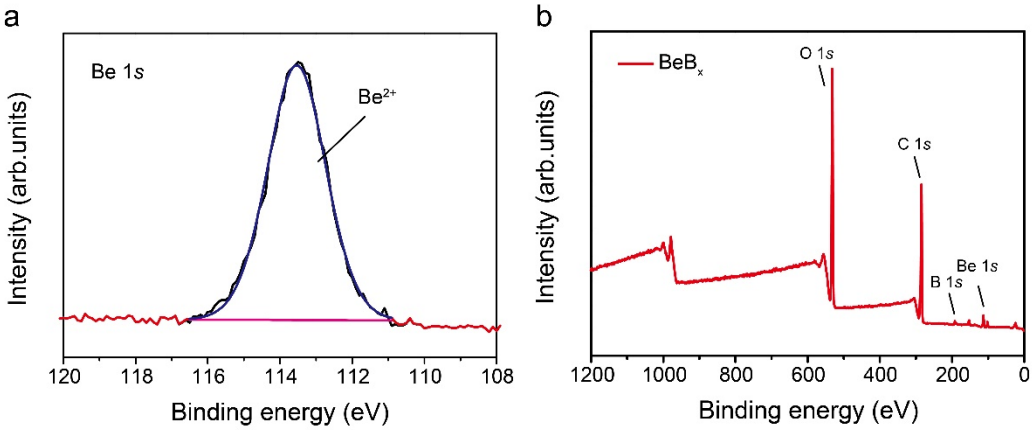

Supplementary Fig. 13 XPS characterization of Nano-BeB_x. **a**, XPS fine spectra of Be 1*s* signal

and **b**, XPS survey spectra of Nano-BeB_x deconvoluted by the multi-Gaussian function.

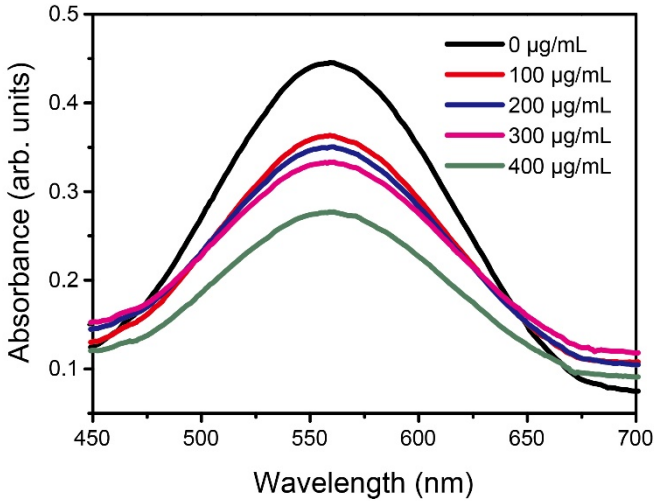

Supplementary Fig. 14 UV-vis spectra of PTIO• scavenging ability with different concentrations of Nano-MgB_2. Data are representative of at least three independent experiments. Source data are provided as a Source Data file.

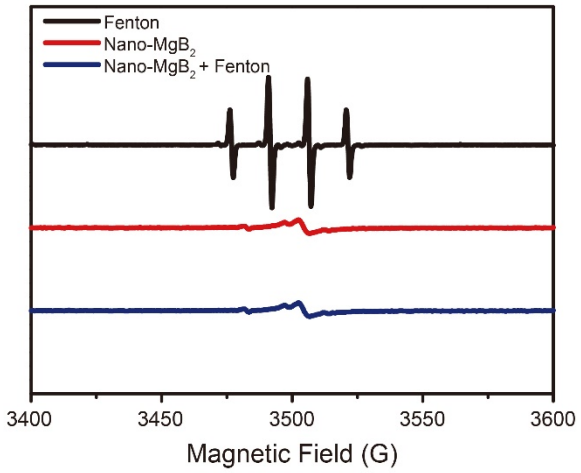

Supplementary Fig. 15 ESR spectra of Nano-MgB_2 under different conditions. Source data are provided as a Source Data file.

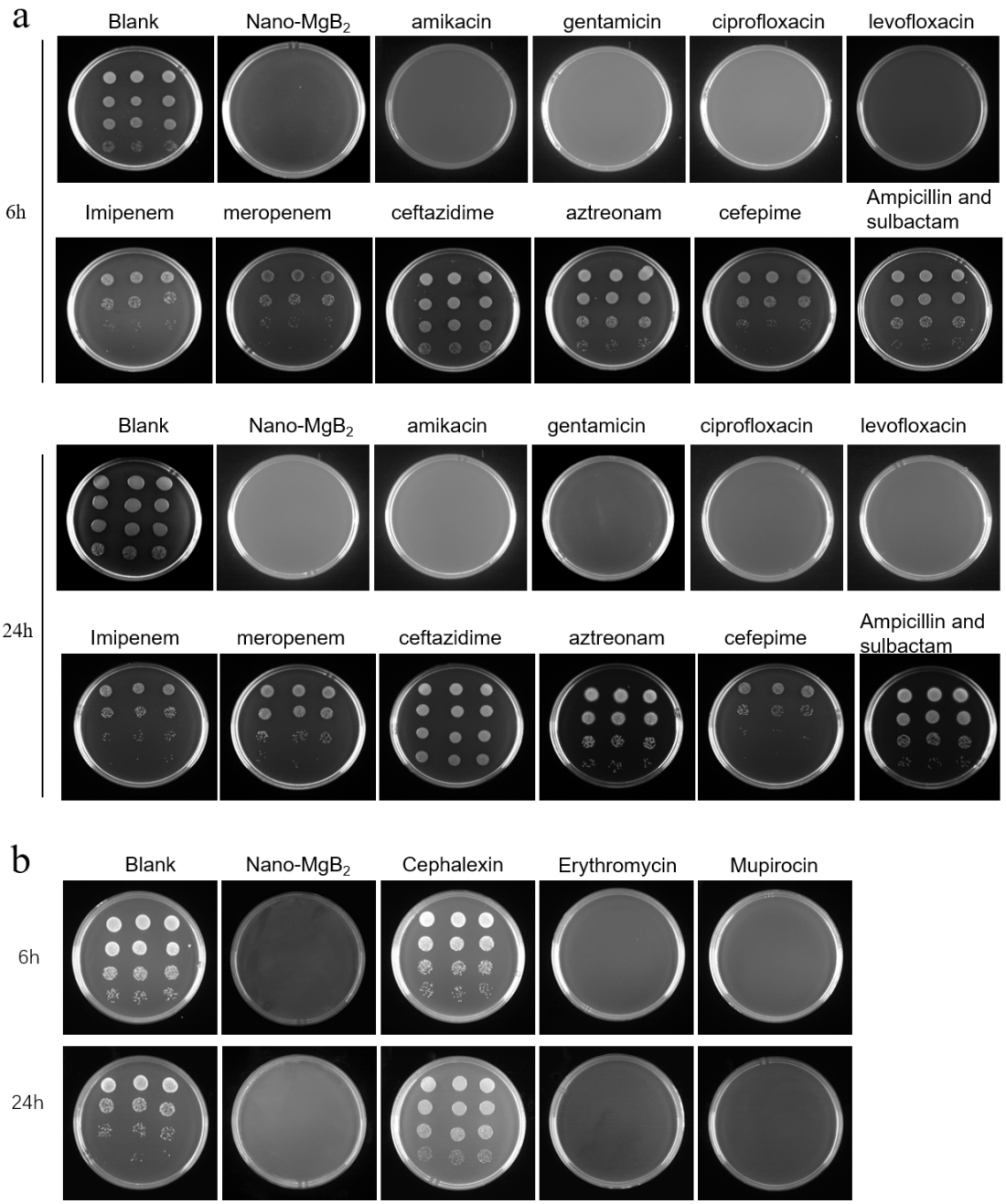

Supplementary Fig. 16 Antibacterial activity of Nano-MgB_2 and antibiotics. **a**, *P. aeruginosa* treated with Nano-MgB_2 (12.5 μg/mL) and different kinds of antibiotics (16 μg/mL) for 6 h and 24 h. **b**, *S. aureus* treated with Nano-MgB_2 (1 mg/mL) and different kinds of antibiotics (1 mg/mL) for 6 h and 24 h (n=3 biological independent cells).

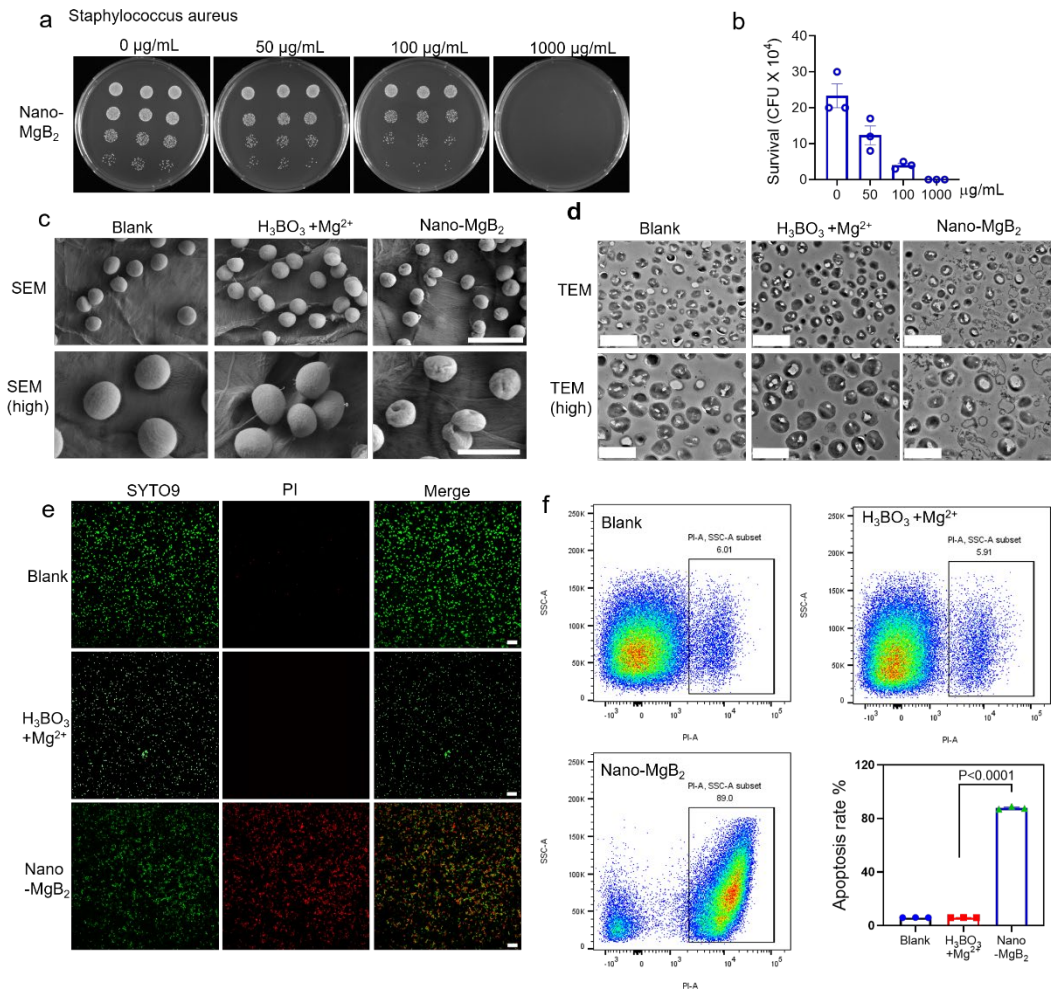

Supplementary Fig. 17 Antibacterial activity of Nano-MgB_2 against *S. aureus*. **a**, *S. aureus* treated with different concentrations of Nano-MgB_2 using colony-forming units counting method. **b**, Survival rates of *S. aureus* taken as in (**a**) (n=3 biologically independent cell). **c**, SEM images of *S. aureus* subjected to Nano-MgB_2 and H_3BO_3+Mg^{2+} Scale bar (up)=2 μm, scale bar (down)=1 μm. **d**, TEM images of *S. aureus* subjected to Nano-MgB_2 and H_3BO_3+Mg^{2+}. Scale bar (up)=2 μm, scale bar (down)=1 μm. **e**, Cell membrane permeability of *S. aureus* treated with Nano-MgB_2 (500 μg/mL) and H_3BO_3+Mg^{2+} by SYTO9 and PI staining. All cells were labelled by the membrane-permeable SYTO9 (green), whereas only cells with damaged membrane were positive for PI (red). Scale bar=20 μm. **f**, FACS analysis of PI-positive bacteria treated as in (**e**) (n=3 biologically independent cells). Data are representative of at least three independent experiments with similar results. Values are the mean ± SEM, one-way ANOVA with Bonferroni post-test was used to analyze multiple groups. Source data are provided as a Source Data file.

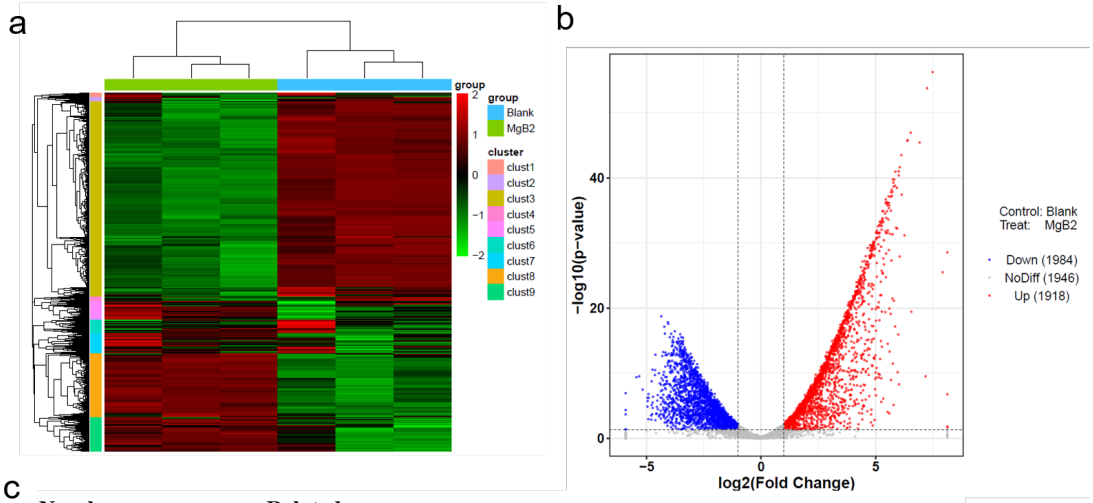

c

Number	Related gene
gene-CIA_RS23525	ATP-dependent DNA helicase RecQ [Pseudomonas aeruginosa PAO1]
gene-CIA_RS29995	Nudix hydrolase YgdP [Pseudomonas aeruginosa]
gene-CIA_RS20225	DNA helicase [Pseudomonas aeruginosa UCBPP-PA14]
gene-CIA_RS26230	hypothetical protein [Pseudomonas sp. 2_1_26]
gene-CIA_RS24915	phosphopyruvate hydratase [Pseudomonas aeruginosa PAO1]
gene-CIA_RS33410	polyphosphate kinase [Pseudomonas aeruginosa UCBPP-PA14]
gene-CIA_RS35865	molecular chaperone DnaK [Pseudomonas aeruginosa PAO1]
gene-CIA_RS36040	poly(A) polymerase [Pseudomonas aeruginosa UCBPP-PA14]
gene-CIA_RS20885	ATP-dependent RNA helicase [Pseudomonas aeruginosa PAO1]
gene-CIA_RS33425	transcription termination factor Rho [Pseudomonas aeruginosa PAO1]
gene-CIA_RS21575	ribonuclease E [Pseudomonas aeruginosa UCBPP-PA14]
gene-CIA_RS34960	exoribonuclease RNase R [Pseudomonas aeruginosa UCBPP-PA14]
gene-CIA_RS29525	ATP-dependent RNA helicase [Pseudomonas aeruginosa UCBPP-PA14]
gene-CIA_RS35975	polynucleotide phosphorylase [Pseudomonas aeruginosa PAO1]
gene-CIA_RS08900	molecular chaperone GroEL [Pseudomonas aeruginosa PAO1]
gene-CIA_RS34920	RNA-binding protein Hfq [Pseudomonas aeruginosa PAO1]

Supplementary Fig. 18. RNA seq of *P. aeruginosa* treated with Nano-MgB_2. **a**, Heat map of differential expressed genes after *P. aeruginosa* treated with Nano-MgB_2. **b**, Volcano plots comparing gene expression after *P. aeruginosa* treated with Nano-MgB_2. The P values were calculated using the negative binomial distribution. **c**, The related gene name of Fig 4j.

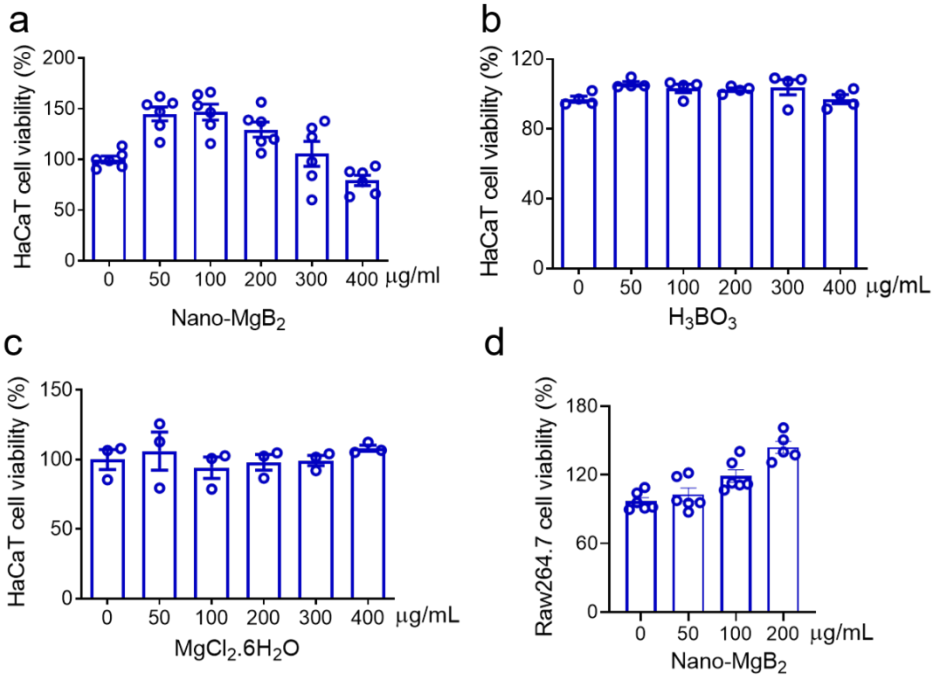

Supplementary Fig. 19 Biocompatibility of Nano-MgB_2. **a-c**, HaCaT cells treated with different concentrations of Nano-MgB_2 (n=6 biologically independent cells), H_3BO_3 (n=4 biologically independent cells) and $MgCl_2$. (n=3 biologically independent cells). **d,** Raw 264.7 cells treated with different concentrations of Nano-MgB_2 (n=5 biologically independent cells). Data are representative of at least three independent experiments with similar results. Values are the mean ± SEM. Source data are provided as a Source Data file.

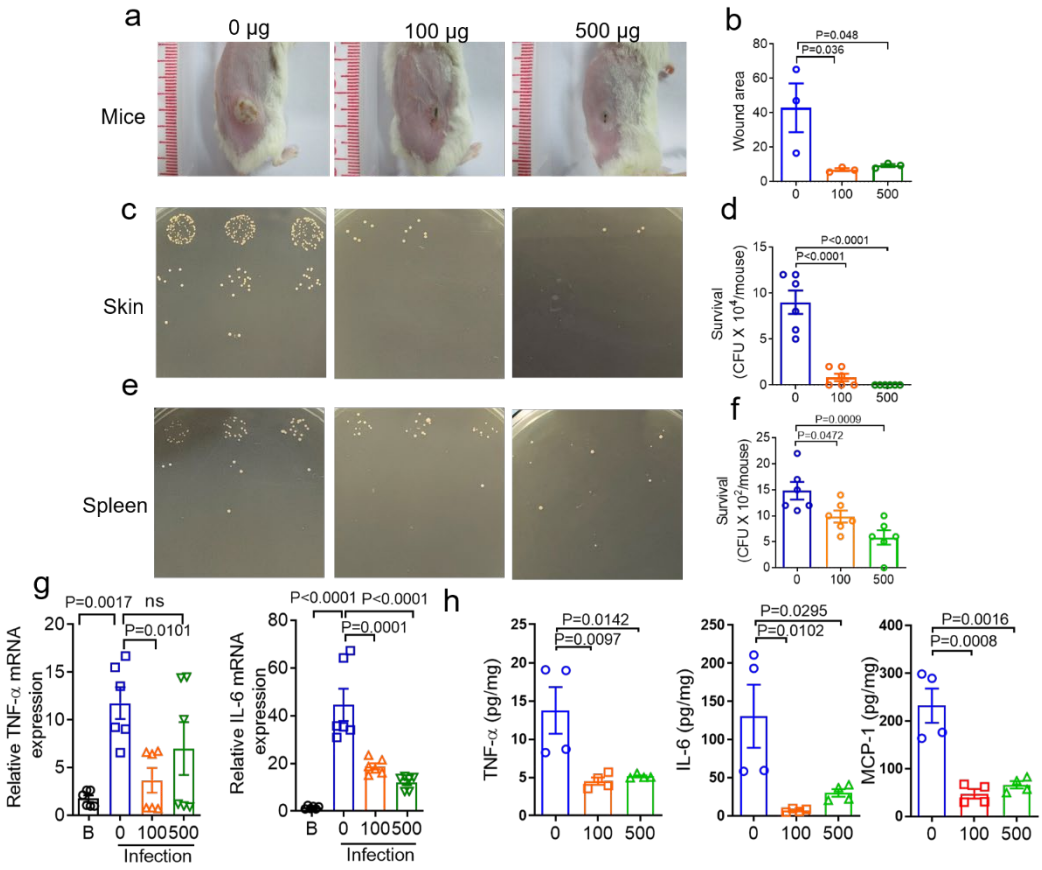

Supplementary Fig. 20 Nano-MgB_2 inhibited *S. aureus*-induced skin infection and inflammation. **a**, Photographs of *S. aureus*-infected mouse skin treated with or without 100 μg and 500 μg/mouse Nano-MgB_2 (n=3 biologically independent mice). **b**, The wound healing rate of mice treated as in (**a**) (n=3 biologically independent mice). **c**, **d**, Survival of bacteria from *S. aureus*-infected mouse skin or (**e**, **f**,) spleen taken as in (**a**) (n=6 biologically independent mice). **g**, QPCR of TNF-α and IL-6 in *S. aureus*-infected mouse skin taken as in (**a**) (n=6 biologically independent mice). **h**, TNF-α, IL-6 and MCP-1 protein expression in *S. aureus*-infected mouse skin taken as in (**a**) (n=4 biologically independent mice). Data are representative of at least three independent experiments with similar results. Values are the mean ± SEM, one-way ANOVA with Bonferroni post test was used to analyze multiple groups. Source data are provided as a Source Data file.

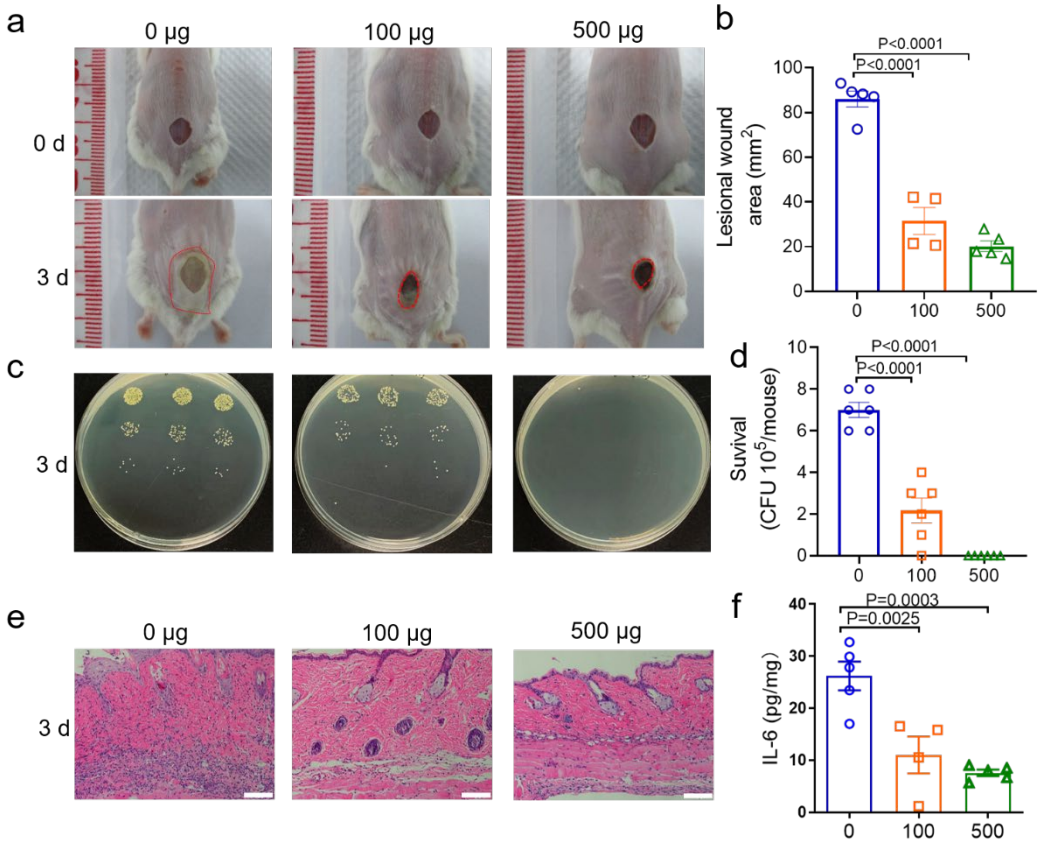

Supplementary Fig. 21. Nano-MgB_2 enhanced *S. aureus*-infected skin wound healing. **a**, Photographs of *S. aureus*-infected skin wounds topically treated with 100 μg and 500 μg/mouse Nano-MgB_2 for 3 days. **b**, The wound healing rate of mice treated as in (**a**) (n=5 biologically independent mice). **c**, **d**, The survival of *S. aureus* in *S. aureus*-infected skin wounds (n=6 biologically independent mice). e, The H&E staining of the infected wound areas (Scale bar=100 μm). **f**, The Inflammatory factor IL-6 protein expression in the lesional skins from mice treated as in (**a**) (n=5 biologically independent mice). Data are representative of at least three independent experiments with similar results. Values are the mean ± SEM, one-way ANOVA with Bonferroni post test was used to analyze multiple groups. Source data are provided as a Source Data file.

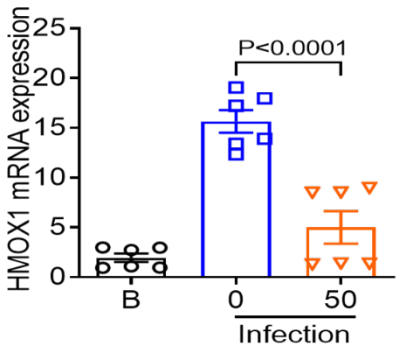

Supplementary Fig. 22. Nano-MgB_2 inhibited oxidative stress-related gene *hmox1* expression in

P. aeruginosa-infected skin wound (n=6 biologically independent mice). Data are representative of at least three independent experiments with similar results. Values are the mean ± SEM, one-way ANOVA with Bonferroni post test was used to analyze multiple groups. Source data are provided as a Source Data file.

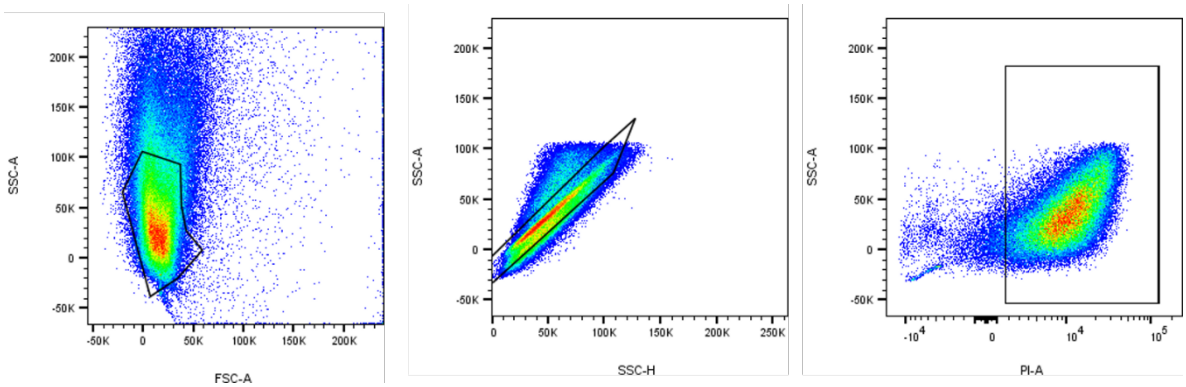

Supplementary Fig. 23 Gating strategy for bacterial Flow Cytometry.

	MB NPs	LPS-binding peptides	Metal nanomaterials	2D antibacterial materials
Materials	Nano-MgB_2 Nano-AlB_2 Nano-BeB_2	Cathelicidins	Silver MgO ZnO	BP MoS_2 hBN
Structure	Hydrolytic 2D materials	Peptide	Low-dimensional materials	2D materials
Function	Anti-microbial Anti-inflammation	Anti-microbial Anti-inflammation	Anti-microbial	Anti-microbial
Mechanisms	(1)Trap LPS or PGN by forming stable borate ester bond (2)Trap LPS or PGN to enhance the local cation concentration, leading to cell membrane damage (3) Trap LPS or PGN to inhibit excessive inflammation	(1) Bind to LPS through electrostatic interaction, leading to cell membrane damage	ROS and Metal cation production	Cell membrane damage Charge transfer ROS production Oxidative stress

Supplementary Table 1 The functional and mechanistic differences among MB NPs, LPS-binding peptides, Metal nanomaterials, and 2D antibacterial materials.

mGAPDH-F	CTTAGCCCCCCTGGCCAAG
mGAPDH-R	TGGTCATGAGCCCTTCCACA
mTNF-α-F	TCAAGGACTCAAATGGGCTTTC
mTNF-α-R	TGCAGAACTCAGGAATGGACAT
mIL-6-F	CTGCAAGAGACTTCCATCCAGTT
mIL-6-R	GGGAAGGCCGTGGTTGTC
mIL-1β-F	TAACCTGTGGCCTTGG
mIL-1β-R	TGTGCTCTGCTTGTGAG
mMCP-1-F	CAGGTCCCTGTCATGCTTCT

mMCP-1-R	GTGGGGCGTTAACTGCATCT
mHmox1-1-F	CAGAACCCAGTCTATGCCCC
mHmox1-1-R	GTGAGGCCCATACCAGAAGG

Supplementary Table 2 QPCR primers for mice.

Pseudomonas aeruginosa UCBPP-PA14 16S F (96bp)	TGCCTGGTAGTGGGGGATAA
Pseudomonas aeruginosa UCBPP-PA14 16S R(96bp)	TCTGATAGCGTGAGGTCCGA
gene-CIA_RS23525 F	GAAGAGCGGGAAATGTGGGA
gene-CIA_RS23525 R	GGGGAAGATCACATAGGGCG
gene-CIA_RS29995 F	ATCAGGAAGCCTGGCAGTTC
gene-CIA_RS29995 R	GCTTGAAGGTCACCACCTGT
gene-CIA_RS20225 F	AGTCCAAGGACGGCCTCTAT
gene-CIA_RS20225 R	CATCAGCCAGGGTATCGACC
gene-CIA_RS26230 F	ATCCACATCGACGGCATCAG
gene-CIA_RS26230 R	ATACGGTGCACGTAGTCGTC
gene-CIA_RS24915 F	AGATCGTCGACATCAAGGGC
gene-CIA_RS24915 R	CAGGATCACGTCCGCTTCAA
gene-CIA_RS33410 F	GACCGATCCGAAGGTCATCC
gene-CIA_RS33410 R	ATCGAGCGCACGTGGATATT
gene-CIA_RS35865 F	GTGATCGAGATCGCCGAAGT
gene-CIA_RS35865 R	GGTAGTCGATCAGGCGGATG
gene-CIA_RS36040 F	GCGACTTCACCATCAATGCC
gene-CIA_RS36040 R	CGATTGCGGATGTCGTGAAC
gene-CIA_RS20885 F	CACAGATCCTCGTCGCTACC
gene-CIA_RS20885 R	TTCCAGGTCGTCCATGAAGC
gene-CIA_RS33425 F	TCTTACGATTCTCGCCACGG
gene-CIA_RS33425 R	TTGATGTTGATGGCCGGGAA
gene-CIA_RS21575 F	CTGAACTTCATCCGCCAGGT
gene-CIA_RS21575 R	CTGGAAGCGATTGAACAGCG
gene-CIA_RS34960 F	CTGGAGAAGATCCACGACCG
gene-CIA_RS34960 R	GAGGTGAAGTGGGTGTAGGC
gene-CIA_RS29525 F	ATCCATGGCAACAAGAGCCA
gene-CIA_RS29525 R	CATGGGGCAACTGGTCGATA
gene-CIA_RS35975 F	CATCAAGCAGGACCGCTACA
gene-CIA_RS35975 R	CAGGCCGAATACGTCCTTGA
gene-CIA_RS08900 F	GTTAAGTTCGGCGATTCCGC
gene-CIA_RS08900 R	ACGACTTGTCCAGAACCACG
gene-CIA_RS34920 F	AGGGCATTCGCTACAAGACC
gene-CIA_RS34920 R	GTCGAAGGACTCGATCTGGC

Supplementary Table 3 QPCR primers for *Pseudomonas aeruginosa.*